

Management of Locally Excited States for Purine-based TADF Emitters: A Method to Reduce Device Efficiency Roll-Off

Yangbo Wu, Yuming Zhang, Chunhao Ran, Jingbo Lan, Zhengyang Bin,* and Jingsong You



Cite This: *Org. Lett.* 2021, 23, 3839–3843



Read Online

ACCESS |



Metrics & More

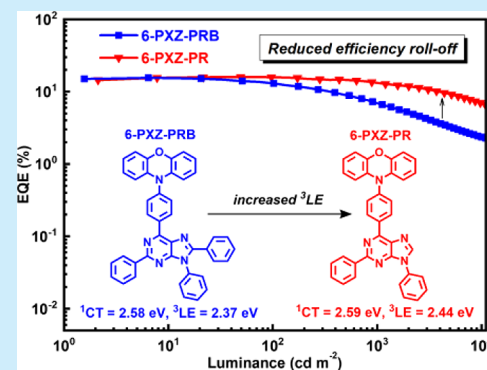


Article Recommendations



Supporting Information

ABSTRACT: The programmed arylation of purine has been developed to construct a series of efficient thermally activated delayed fluorescent (TADF) materials. The corresponding organic light-emitting diodes (OLEDs) exhibit external quantum efficiency as high as 16.0% alongside small efficiency roll-off. Intriguingly, this work proves that the good management of localized states is an efficient way to reduce device efficiency roll-off and is crucial for the future design of high-performance OLEDs.



Thermally activated delayed fluorescent (TADF) materials that possess small singlet–triplet energy gaps (ΔE_{ST}) so as to efficiently upconvert “dark” triplet excitons to emissive singlet excitons have received tremendous research interests in recent years and have been considered as the next generation of emitters in organic light-emitting diodes (OLEDs).^{1–5} A typical molecular design concept for efficient TADF materials is to construct compounds by bridging electron-rich donors (D) and electron-deficient acceptors (A) with highly twisted phenyl linkages.^{6–8} The twisted D– π –A conformation can ensure well-separated highest occupied molecular orbital (HOMO) and lowest unoccupied molecular orbital (LUMO) distributions, thus leading to a small ΔE_{ST} value alongside a fast reverse intersystem crossing rate (k_{risc}) for an efficient triplet exciton utilization process.^{9,10}

As reported, electron-deficient nitrogen-containing heterocycles are well-documented as acceptors for developing efficient TADF materials.^{11–13} On one hand, the high electron deficiency of these heterocyclic structures can lead to small ΔE_{ST} values when TADF materials are formed; meanwhile, heterocyclic structures are also favorable for forming intermolecular hydrogen bonding between the nitrogen atoms and the phenyl linkage, so as to inhibit structure relaxation and increase the photoluminescence quantum yield (PLQY).^{14–16} For example, triazine (TRZ) that features a hexagonal heterocycle is one of the most widely used electron acceptors and has shown great success in assembling a large amount of TADF materials.^{17–19} Recently, by fusing a pentagonal triazole (TAZ) unit on TRZ acceptor, we have developed a new type of triazolotriazine (TAZTRZ) acceptor and constructed a series of highly efficient TADF materials to

realize state-of-the-art-performance yellow fluorescent OLEDs.²⁰

As a naturally occurring moiety, the purine unit also possesses a unique structure with a fused hexagonal pyrimidine and pentagonal imidazole, which provides us with an opportunity to further investigate the performance of a nitrogen-containing heterocyclic acceptor in assembling efficient TADF materials.^{21–23} By introducing a phenoxazine (PXZ) donor at a different location of the purine acceptor through the programmed arylation reaction, we herein wish to design and synthesize a series of purine-based TADF materials (2-PXZ-PRB, 6-PXZ-PRB, 8-PXZ-PRB, 2-PXZ-PR, and 6-PXZ-PR, Figure 1) and then systematically investigate their photoluminescence (PL) and electroluminescence (EL) performance.

To understand the structure–property relationship of these compounds at the molecular level, density functional theory (DFT) and time-dependent DFT (TD-DFT) calculations were performed to study the electronic states and the distributions of their frontier molecular orbitals (FMOs). As shown in Figure 1, because of the large dihedral angles of almost 90° between the PXZ donor and the phenyl bridge, all molecules have well-separated FMO distributions, where the HOMOs and the LUMOs are mainly localized on the electron-rich PXZ

Received: March 17, 2021

Published: May 7, 2021



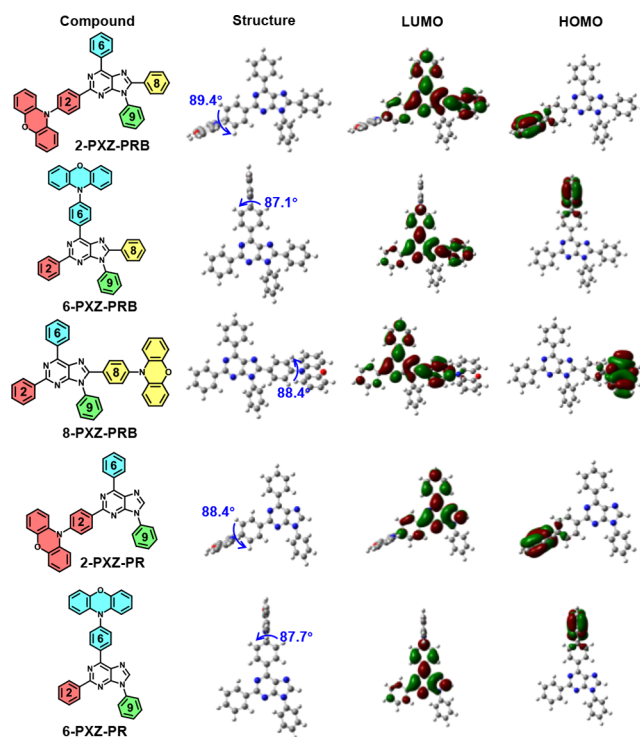


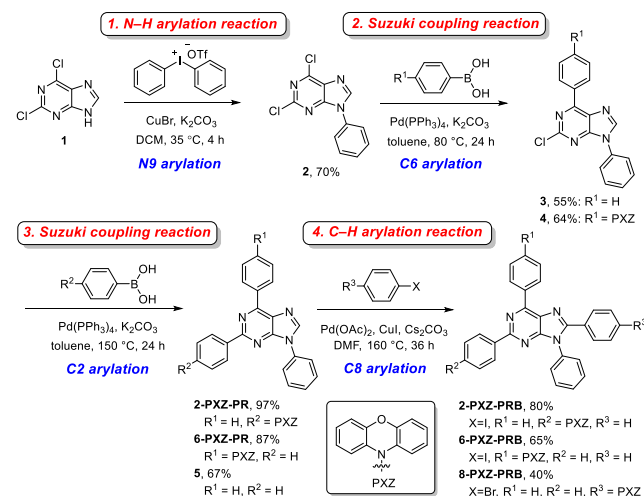
Figure 1. Molecular structures and FMO distributions of 2-PXZ-PRB, 6-PXZ-PRB, 8-PXZ-PRB, 2-PXZ-PR, and 6-PXZ-PR.

and electron-deficient purine units, respectively. Therefore, this leads to small ΔE_{ST} values of 0.0032, 0.0078, 0.0066, 0.0048, and 0.0070 eV for 2-PXZ-PRB, 6-PXZ-PRB, 8-PXZ-PRB, 2-PXZ-PR, and 6-PXZ-PR, respectively, which indicates their potential TADF nature. Notably, around the purine acceptor, there is almost no LUMO distribution on the phenyl ring that is bonded to the electron-rich nitrogen atom at the nine-position, indicating the limited influence of this phenyl ring on the FMO energy level alignment for the targeting TADF materials.

2-PXZ-PRB, 6-PXZ-PRB, 8-PXZ-PRB, 2-PXZ-PR, and 6-PXZ-PR were synthesized via the programmed arylation reactions, as shown in Scheme 1. The N9-arylation of purine was first realized by the Cu-catalyzed N–H arylation reaction to deliver compound 2 in 70% yield;²⁴ then, Suzuki cross-coupling reactions were rapidly carried out to afford 2-PXZ-PR, 6-PXZ-PR, and the intermediate compound 5.^{25,26} Crucially, the regioselective C2-arylation and C6-arylation were accomplished at different temperatures, 80 °C for C6-arylation and 150 °C for C2-arylation. Finally, the palladium-catalytic C–H arylation reaction was successfully used to realize C8-arylation in the presence of CuI and Cs₂CO₃, furnishing 2-PXZ-PRB, 6-PXZ-PRB, and 8-PXZ-PRB in yields of 80, 65, and 40%, respectively.^{27,28}

Cyclic voltammetry (CV) measurements were used to investigate the electrochemical properties of these compounds. As shown in Figure S3, all molecules exhibit clearly reversible and similar oxidation processes that originated from the same PXZ donor of these compounds. The HOMO energy levels are therefore calculated to be the same as –5.05 eV according to the oxidation peaks in the CV curves; meanwhile, their LUMO energy levels are calculated from the HOMO energy levels and the optical energy gaps obtained from the absorption spectra, which are determined to be –2.28 eV for 2-PXZ-PRB, –2.44

Scheme 1. Programmed Arylation of Purine for the Synthesis of 2-PXZ-PRB, 6-PXZ-PRB, 8-PXZ-PRB, 2-PXZ-PR, and 6-PXZ-PR



eV for 6-PXZ-PRB, –2.40 eV for 8-PXZ-PRB, –2.30 eV for 2-PXZ-PR, and –2.45 eV for 6-PXZ-PR, respectively. Subsequently, thermogravimetric analysis (TGA) and differential scanning calorimetry (DSC) measurements were carried out to investigate the thermal properties of these compounds (Figure S4). These compounds all possess high decomposition temperatures (T_d , which is the temperature for 5% weight loss) of 432, 425, 428, 416, and 417 °C and high glass-transition temperatures (T_g) of 143, 139, 133, 120, and 116 °C for 2-PXZ-PRB, 6-PXZ-PRB, 8-PXZ-PRB, 2-PXZ-PR, and 6-PXZ-PR, respectively. The sufficiently high T_d and T_g values of these compounds reveal their high thermal stability, which makes them good candidates for vacuum-possessed OLED materials.

To investigate the PL properties of 2-PXZ-PRB, 6-PXZ-PRB, 8-PXZ-PRB, 2-PXZ-PR, and 6-PXZ-PR, UV–vis absorption spectra (Abs), fluorescence spectra (FL) at room temperature, and phosphorescence spectra at 77 K with a delay time of 10 ms were measured in dilute toluene (1×10^{-5} mol L⁻¹). As depicted in Figure 2a, all of the compounds exhibit similar broad absorption bands from 380 to 480 nm, which are attributed to the intramolecular charge-transfer transition from PXZ donors to purine acceptors. As shown in the FL spectra, these compounds all show broad and featureless emissions from 490 to 535 nm, indicating that their singlet excitons belong to charge-transfer states (¹CT).²⁹ Therefore, the ¹CT energies of 2-PXZ-PRB, 6-PXZ-PRB, 8-PXZ-PRB, 2-PXZ-PR, and 6-PXZ-PR were calculated from the onset wavelengths of the FL spectra.

As summarized in Table 1, 2-PXZ-PRB, 6-PXZ-PRB, and 8-PXZ-PRB that have different donor–acceptor linkages possess different ¹CT energies, which are 2.75, 2.58, and 2.66 eV, respectively; meanwhile, the phenyl ring on the C8 position of the purine unit would only slightly change the ¹CT energy, revealing the limited influence of this phenyl ring on charge-transfer characteristics. As shown in Figure 2b, the phosphorescence spectra of these compounds all show clearly vibrational structures, indicating that their triplet excitons belong to localized excited states (³LE), which can also be demonstrated by the natural transition orbital calculation results (Table S5). The ³LE energies can be obtained from the emission peaks in the short-wavelength region of phosphor-

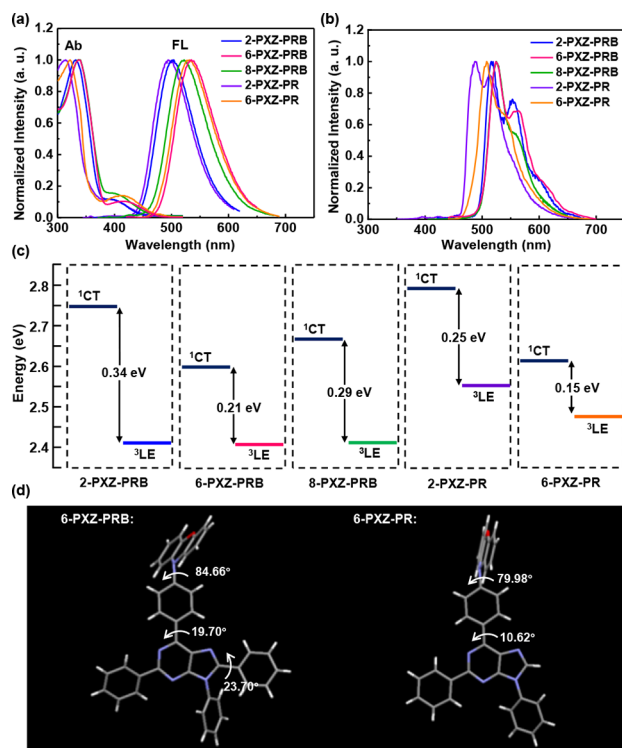


Figure 2. (a) Absorption (Ab) and fluorescence (FL) spectra measured at room temperature and (b) phosphorescence spectra measured at 77 K with a delay time of 10 ms of 2-PXZ-PRB, 6-PXZ-PRB, 8-PXZ-PRB, 2-PXZ-PR, and 6-PXZ-PR in dilute toluene (1×10^{-5} mol L $^{-1}$). (c) ^1CT and ^3LE energy level alignments of 2-PXZ-PRB, 6-PXZ-PRB, 8-PXZ-PRB, 2-PXZ-PR, and 6-PXZ-PR. (d) Crystal structures of 6-PXZ-PRB and 6-PXZ-PR.

escence spectra.^{30,31} As summarized in Table 1 and depicted in Figure 2c, although the ^1CT energies of 6-PXZ-PRB (2.58 eV) and 6-PXZ-PR (2.59 eV) are similar, the ^3LE energy of 6-PXZ-PR (2.44 eV) is significantly higher than that of 6-PXZ-PRB (2.37 eV). This leads to a smaller $\Delta E_{(^1\text{CT}-^3\text{LE})}$ of 6-PXZ-PR (0.15 eV) than that of 6-PXZ-PRB (0.21 eV). A similar phenomenon is seen for 2-PXZ-PRB and 2-PXZ-PR. The crystal structures of 6-PXZ-PRB and 6-PXZ-PR are obtained by the temperature gradient vacuum sublimation method (Figures S1 and S2). As shown in Figure 2d, a small dihedral angle of 23.7° of the purine–phenyl (ring 8) linkage is observed in the crystal structure of 6-PXZ-PRB, which is indicative of its extended π -conjugation length at the C8 position compared with that of 6-PXZ-PR, which increases the ^3LE energy.^{32,33} The $\Delta E_{(^1\text{CT}-^3\text{LE})}$ energies of 2-PXZ-PRB, 6-PXZ-PRB, 8-PXZ-PRB, 2-PXZ-PR, and 6-PXZ-PR are

summarized in Table 1, which are 0.34, 0.21, 0.29, 0.25, and 0.15 eV, respectively, indicating that these compounds all have good TADF nature, as calculated. In addition, the FL spectra (Figure S5) and transient PL spectra (Figure S6) of these compounds are also measured in the doped film of the 3,3'-bis(carbazol-9-yl)biphenyl (mCBP) host. The transient PL spectra show an obvious delayed component with an average delayed lifetime (τ_d) of 58.5, 48.1, 43.4, 32.5, and 24.3 μs , respectively. Furthermore, the radiative decay rate (k_r) and k_{risc} are calculated and summarized in Table S7. Compared with 6-PXZ-PRB, the significantly increased k_{risc} and the slightly decreased k_r lead to a large PLQY (Φ_{PL}) for 6-PXZ-PR (Table 1), rendering it a good TADF emitter.

To further explore the EL performance of these compounds, we have designed and assembled multilayer OLED devices with the optimized device structure of ITO/HAT-CN (5 nm)/NPB (30 nm)/TCTA (5 nm)/20% emitter:mCBP (30 nm)/TmPyPb (40 nm)/LiF (0.8 nm)/Al (100 nm), in which 2-PXZ-PRB, 6-PXZ-PRB, 8-PXZ-PRB, 2-PXZ-PR, and 6-PXZ-PR are separately used as the emitters in the mCBP host. The molecular structures, energy diagrams, and EL characteristics of the OLED devices are shown in Figure 3. The device

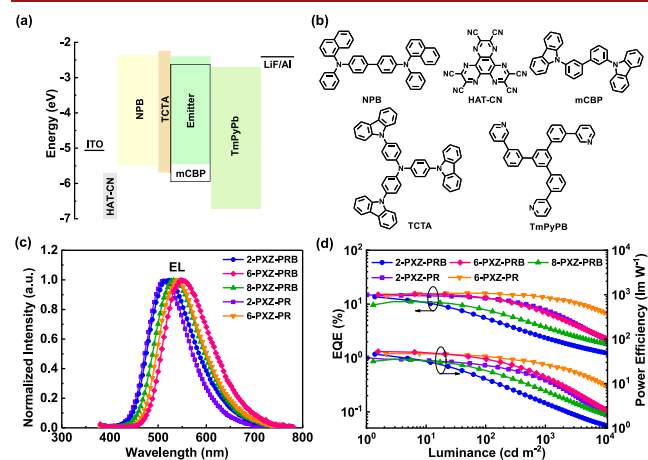


Figure 3. Device performance. (a) Device structures. (b) Molecular structures used in OLED devices. (c) EL spectra at 5000 cd m $^{-2}$. (d) EQE–luminance and power efficiency–luminance characteristics of 2-PXZ-PRB-, 6-PXZ-PRB-, 8-PXZ-PRB-, 2-PXZ-PR-, and 6-PXZ-PR-based OLEDs.

performance is summarized in Table 2. OLEDs devices based on 2-PXZ-PRB, 6-PXZ-PRB, and 8-PXZ-PRB that feature a PXZ donor at a different position of the purine acceptor exhibit green to yellow emission with emission peaks of 518, 550, and 530 nm, respectively. Moreover, 6-PXZ-PRB that

Table 1. Summary of Thermal and Photophysical Properties of 2-PXZ-PRB, 6-PXZ-PRB, 8-PXZ-PRB, 2-PXZ-PR, and 6-PXZ-PR

compound	T_d/T_g (°C)	$\lambda_{\text{abs}}/\lambda_{\text{em}}$ (nm) ^a	^1CT (eV) ^b	^3LE (eV) ^c	$\Delta E_{(^1\text{CT}-^3\text{LE})}$ (eV) ^d	Φ_{PL} (%) ^e
2-PXZ-PRB	432/143	389/504	2.75	2.41	0.34	24.8
6-PXZ-PRB	425/139	415/535	2.58	2.37	0.21	37.6
8-PXZ-PRB	428/133	400/522	2.66	2.37	0.29	27.2
2-PXZ-PR	416/120	392/494	2.80	2.55	0.25	20.2
6-PXZ-PR	417/116	413/531	2.59	2.44	0.15	60.8

^aMeasured in dry toluene solution (1×10^{-5} mol L $^{-1}$). ^bEstimated from the onset of the fluorescence spectra measured at room temperature in toluene solution (1×10^{-5} mol L $^{-1}$). ^cEstimated from the phosphorescence spectra measured at 77 K in toluene solution (1×10^{-5} mol L $^{-1}$). ^dCalculated from ^1CT and ^3LE . ^ePLQY (Φ_{PL}) measured in mCBP films.

Table 2. Summary of Device Performances

emitter	λ_{EL} (nm)	V_{on} (V) ^a	EQE_{max} (%) ^b	PE_{max} (lm W ⁻¹) ^c	EQE/PE (at 1000 cd m ⁻²)	EQE/PE (at 5000 cd m ⁻²)
2-PXZ-PRB	518	2.7	13.6	45.8	2.4/3.6	1.5/1.6
6-PXZ-PRB	550	2.8	15.5	52.6	6.9/13.9	3.2/4.5
8-PXZ-PRB	530	3.0	11.1	35.1	3.7/6.7	2.2/2.8
2-PXZ-PR	510	3.5	14.9	38.1	7.8/11.9	3.3/3.6
6-PXZ-PR	541	3.1	16.0	47.5	13.1/26.5	9.2/14.4

^aTurn-on voltage measured at 1 cd m⁻². ^bExternal quantum efficiency. ^cPower efficiency.

features a PXZ donor at the C6-position of the purine acceptor displays a relatively better EL performance with a higher EQE_{max} of 15.5% compared with those of 2-PXZ-PRB (13.6%) and 8-PXZ-PRB (11.1%). However, devices based on 2-PXZ-PRB, 6-PXZ-PRB, and 8-PXZ-PRB emitters all suffer from serious efficiency roll-off. For example, at a luminance of 1000 cd m⁻², the EQEs of 2-PXZ-PRB, 6-PXZ-PRB, and 8-PXZ-PRB rapidly dropped to 2.4, 6.9, and 3.7%, respectively. The severe efficiency roll-off is mainly due to the accumulation of triplet excitons in the emitting layer.³⁴ As discussed, moving out a benzene ring at the C8-position can significantly increase the energy level of ³LE, and thus it enhances the up-conversion process of triplet excitons and inhibits the triplet exciton quenching, which is beneficial for reducing the efficiency roll-off. Therefore, compared with 2-PXZ-PRB- and 6-PXZ-PRB-based devices, devices using 2-PXZ-PR and 6-PXZ-PR as the emitter exhibit remarkably reduced efficiency roll-off. For instance, 2-PXZ-PR- and 6-PXZ-PR-based devices display EQE_{max} values of 14.9 and 16.0%, respectively, which are comparable with those of 2-PXZ-PRB-based device (13.6%) and 6-PXZ-PRB-based device (15.5%). However, at a luminance of 1000 cd m⁻², the EQE_{1000} values of 2-PXZ-PR- and 6-PXZ-PR-based devices can be maintained at 7.8 and 13.1%, respectively, which are significantly higher than those of the 2-PXZ-PRB-based device (2.4%) and the 6-PXZ-PRB-based device (6.9%). Crucially, even at a luminance of 5000 cd m⁻², the EQE_{5000} of the 6-PXZ-PR-based device can still be maintained at 9.2%, indicating a significantly reduced efficiency roll-off.

In conclusion, we designed and synthesized a series of purine-based TADF materials (2-PXZ-PRB, 6-PXZ-PRB, 8-PXZ-PRB, 2-PXZ-PR, and 6-PXZ-PR) that exhibit good PL performance with emission peaks from 494 to 535 nm and $\Delta E_{(\text{ICT-}^3\text{LE})}$ values as small as 0.15 eV. Moreover, these compounds also achieve good EL performance with turn-on voltage as low as 2.7 V and EQE_{max} as high as 16.0%. Crucially, this work demonstrates that the good management of ³LE states in TADF emitters is an efficient way to reduce device efficiency roll-off and is important for the future design of high-performance OLED devices associated with TADF materials.

■ ASSOCIATED CONTENT

Supporting Information

The Supporting Information is available free of charge at <https://pubs.acs.org/doi/10.1021/acs.orglett.1c00918>.

Experimental details, additional spectra and data, and copies of ¹H and ¹³C NMR spectra of products (PDF)

Accession Codes

CCDC 2069564 and 2069566 contain the supplementary crystallographic data for this paper. These data can be obtained free of charge via www.ccdc.cam.ac.uk/data_request/cif, or by emailing data_request@ccdc.cam.ac.uk, or by contacting The

Cambridge Crystallographic Data Centre, 12 Union Road, Cambridge CB2 1EZ, UK; fax: +44 1223 336033.

■ AUTHOR INFORMATION

Corresponding Author

Zhengyang Bin – Key Laboratory of Green Chemistry and Technology of Ministry of Education, College of Chemistry, Sichuan University, Chengdu 610064, P. R. China;
 orcid.org/0000-0001-6216-7234;
 Email: binzhengyang@scu.edu.cn

Authors

Yangbo Wu – Key Laboratory of Green Chemistry and Technology of Ministry of Education, College of Chemistry, Sichuan University, Chengdu 610064, P. R. China
 Yuming Zhang – Key Laboratory of Green Chemistry and Technology of Ministry of Education, College of Chemistry, Sichuan University, Chengdu 610064, P. R. China
 Chunhao Ran – Key Laboratory of Green Chemistry and Technology of Ministry of Education, College of Chemistry, Sichuan University, Chengdu 610064, P. R. China
 Jingbo Lan – Key Laboratory of Green Chemistry and Technology of Ministry of Education, College of Chemistry, Sichuan University, Chengdu 610064, P. R. China;
 orcid.org/0000-0001-5937-0987
 Jingsong You – Key Laboratory of Green Chemistry and Technology of Ministry of Education, College of Chemistry, Sichuan University, Chengdu 610064, P. R. China;
 orcid.org/0000-0002-0493-2388

Complete contact information is available at:
<https://pubs.acs.org/doi/10.1021/acs.orglett.1c00918>

Notes

The authors declare no competing financial interest.

■ ACKNOWLEDGMENTS

We acknowledge financial support from the National NSF of China (nos. 22031007 and 22005204) and the Sichuan Science and Technology Program (nos. 2020YJ0245 and 2020YJ0302). We also thank the Comprehensive Training Platform Specialized Laboratory, College of Chemistry, Sichuan University.

■ REFERENCES

- (1) Uoyama, H.; Goushi, K.; Shizu, K.; Nomura, H.; Adachi, C. Highly Efficient Organic Light-Emitting Diodes from Delayed Fluorescence. *Nature* **2012**, *492*, 234–238.
- (2) Goushi, K.; Yoshida, K.; Sato, K.; Adachi, C. Organic Light-Emitting Diodes Employing Efficient Reverse Intersystem Crossing for Triplet-to-Singlet State Conversion. *Nat. Photonics* **2012**, *6*, 253–258.
- (3) Liang, W.; Yang, Y.; Yang, M.; Zhang, M.; Li, C.; Ran, Y.; Lan, J.; Bin, Z.; You, J. Dearomatizing [4 + 1] Spiroannulation of Naphthols:

Discovery of Thermally Activated Delayed Fluorescent Materials. *Angew. Chem., Int. Ed.* **2021**, *60*, 3493–3497.

(4) Huang, Z.; Bin, Z.; Su, R.; Yang, F.; Lan, J.; You, J. Molecular Design of Non-Doped OLEDs Based on a Twisted Heptagonal Acceptor: A Delicate Balance between Rigidity and Rotatability. *Angew. Chem., Int. Ed.* **2020**, *59*, 9992–9996.

(5) Liu, Y.; Li, C.; Ren, Z.; Yan, S.; Bryce, M. R. All-Organic Thermally Activated Delayed Fluorescence Materials for Organic Light-Emitting Diodes. *Nat. Rev. Mater.* **2018**, *3*, 18020.

(6) Rao, J.; Yang, L.; Li, X.; Zhao, L.; Wang, S.; Ding, J.; Wang, L. Meta Junction Promoting Efficient Thermally Activated Delayed Fluorescence in Donor-Acceptor Conjugated Polymers. *Angew. Chem., Int. Ed.* **2020**, *59*, 17903–17909.

(7) Peng, C. C.; Yang, S. Y.; Li, H. C.; Xie, G. H.; Cui, L. S.; Zou, S. N.; Poriel, C.; Jiang, Z. Q.; Liao, L. S. Highly Efficient Thermally Activated Delayed Fluorescence Via an Unconjugated Donor-Acceptor System Realizing η_{eq} of over 30. *Adv. Mater.* **2020**, *32*, 2003885.

(8) Izumi, S.; Higginbotham, H. F.; Nyga, A.; Stachelek, P.; Tohnai, N.; Silva, P.; Data, P.; Takeda, Y.; Minakata, S. Thermally Activated Delayed Fluorescent Donor-Acceptor-Donor-Acceptor π -Conjugated Macrocycle for Organic Light-Emitting Diodes. *J. Am. Chem. Soc.* **2020**, *142*, 1482–1491.

(9) Zhang, Q.; Kuwabara, H.; Potscavage, W. J., Jr.; Huang, S.; Hatae, Y.; Shibata, T.; Adachi, C. Anthraquinone-Based Intramolecular Charge-Transfer Compounds: Computational Molecular Design, Thermally Activated Delayed Fluorescence, and Highly Efficient Red Electroluminescence. *J. Am. Chem. Soc.* **2014**, *136*, 18070–18081.

(10) Cui, L. S.; Nomura, H.; Geng, Y.; Kim, J. U.; Nakanotani, H.; Adachi, C. Controlling Singlet-Triplet Energy Splitting for Deep-Blue Thermally Activated Delayed Fluorescence Emitters. *Angew. Chem., Int. Ed.* **2017**, *56*, 1571–1575.

(11) Jayakumar, J.; Wu, T. L.; Huang, M. J.; Huang, P. Y.; Chou, T. Y.; Lin, H. W.; Cheng, C. H. Pyridine-Carbonitrile-Carbazole-Based Delayed Fluorescence Materials with Highly Congested Structures and Excellent OLED Performance. *ACS Appl. Mater. Interfaces* **2019**, *11*, 21042–21048.

(12) Congrave, D. G.; Drummond, B. H.; Conaghan, P. J.; Francis, H.; Jones, S. T. E.; Grey, C. P.; Greenham, N. C.; Credgington, D.; Bronstein, H. A Simple Molecular Design Strategy for Delayed Fluorescence toward 1000 Nm. *J. Am. Chem. Soc.* **2019**, *141*, 18390–18394.

(13) Xue, J.; Liang, Q.; Wang, R.; Hou, J.; Li, W.; Peng, Q.; Shuai, Z.; Qiao, J. Highly Efficient Thermally Activated Delayed Fluorescence Via J-Aggregates with Strong Intermolecular Charge Transfer. *Adv. Mater.* **2019**, *31*, 1808242.

(14) Qiu, W.; Cai, X.; Li, M.; Wang, L.; He, Y.; Xie, W.; Chen, Z.; Liu, M.; Su, S.-J. Dynamic Adjustment of Emission from Both Singlets and Triplets: The Role of Excited State Conformation Relaxation and Charge Transfer in Phenothiazine Derivates. *J. Mater. Chem. C* **2021**, *9*, 1378–1386.

(15) Rajamalli, P.; Senthilkumar, N.; Huang, P. Y.; Ren-Wu, C. C.; Lin, H. W.; Cheng, C. H. New Molecular Design Concurrently Providing Superior Pure Blue, Thermally Activated Delayed Fluorescence and Optical out-Coupling Efficiencies. *J. Am. Chem. Soc.* **2017**, *139*, 10948–10951.

(16) Shi, Y.; Wang, K.; Tsuchiya, Y.; Liu, W.; Komino, T.; Fan, X.; Sun, D.; Dai, G.; Chen, J.; Zhang, M.; Zheng, C.; Xiong, S.; Ou, X.; Yu, J.; Jie, J.; Lee, C.-S.; Adachi, C.; Zhang, X. Hydrogen Bond-Modulated Molecular Packing and Its Applications in High-Performance Non-Doped Organic Electroluminescence. *Mater. Horiz.* **2020**, *7*, 2734–2740.

(17) Endo, A.; Sato, K.; Yoshimura, K.; Kai, T.; Kawada, A.; Miyazaki, H.; Adachi, C. Efficient up-Conversion of Triplet Excitons into a Singlet State and Its Application for Organic Light Emitting Diodes. *Appl. Phys. Lett.* **2011**, *98*, 083302.

(18) Lin, T. A.; Chatterjee, T.; Tsai, W. L.; Lee, W. K.; Wu, M. J.; Jiao, M.; Pan, K. C.; Yi, C. L.; Chung, C. L.; Wong, K. T.; Wu, C. C.

Sky-Blue Organic Light Emitting Diode with 37% External Quantum Efficiency Using Thermally Activated Delayed Fluorescence from Spiroacridine-Triazine Hybrid. *Adv. Mater.* **2016**, *28*, 6976–6983.

(19) Nguyen, T. B.; Nakanotani, H.; Hatakeyama, T.; Adachi, C. The Role of Reverse Intersystem Crossing Using a TADF-Type Acceptor Molecule on the Device Stability of Exciplex-Based Organic Light-Emitting Diodes. *Adv. Mater.* **2020**, *32*, 1906614.

(20) Su, R.; Zhao, Y.; Yang, F.; Duan, L.; Lan, J.; Bin, Z.; You, J. Triazolotriazine-Based Thermally Activated Delayed Fluorescence Materials for Highly Efficient Fluorescent Organic Light-Emitting Diodes (TSF-OLEDs). *Sci. Bull.* **2021**, *66*, 441–448.

(21) Yang, Y.; Cohn, P.; Eom, S.-H.; Abboud, K. A.; Castellano, R. K.; Xue, J. Ultraviolet-Violet Electroluminescence from Highly Fluorescent Purines. *J. Mater. Chem. C* **2013**, *1*, 2867–2874.

(22) Wang, Z.; Yao, J.; Zhan, L.; Gong, S.; Ma, D.; Yang, C. Purine-Based Thermally Activated Delayed Fluorescence Emitters for Efficient Organic Light-Emitting Diodes. *Dyes Pigm.* **2020**, *180*, 108437.

(23) Yao, J.; Wang, Z.; Qiao, X.; Yang, D.; Dai, Y.; Sun, Q.; Chen, J.; Yang, C.; Ma, D. High Efficiency and Long Lifetime Fluorescent Organic Light-Emitting Diodes Based on Cascaded Energy Transfer Processes to Efficiently Utilize Triplet Excitons Via Sensitizer. *Org. Electron.* **2020**, *84*, 105824.

(24) Niu, H. Y.; Xia, C.; Qu, G. R.; Zhang, Q.; Jiang, Y.; Mao, R. Z.; Li, D. Y.; Guo, H. M. CuBr Catalyzed C-N Cross Coupling Reaction of Purines and Diaryliodonium Salts to 9-Arylpurines. *Org. Biomol. Chem.* **2011**, *9*, 5039–5042.

(25) Cerna, I.; Pohl, R.; Klepetarova, B.; Hocek, M. Synthesis of 6,8,9-Tri- and 2,6,8,9-Tetrasubstituted Purines by a Combination of the Suzuki Cross-Coupling, N-Arylation, and Direct C-H Arylation Reactions. *J. Org. Chem.* **2008**, *73*, 9048–9054.

(26) Chang, L. C. W.; Spanjersberg, R. F.; von Frijtag Drabbe Künzel, J. K.; Mulder-Krieger, T.; Brussee, J.; Ijzerman, A. P. 2,6-Disubstituted and 2,6,8-Trisubstituted Purines as Adenosine Receptor Antagonists. *J. Med. Chem.* **2006**, *49*, 2861–2867.

(27) Zhao, D.; Wang, W.; Yang, F.; Lan, J.; Yang, L.; Gao, G.; You, J. Copper-Catalyzed Direct C Arylation of Heterocycles with Aryl Bromides: Discovery of Fluorescent Core Frameworks. *Angew. Chem., Int. Ed.* **2009**, *48*, 3296–3300.

(28) Čerňa, I.; Pohl, R.; Klepetářová, B.; Hocek, M. Direct C–H Arylation of Purines: Development of Methodology and Its Use in Regioselective Synthesis of 2,6,8-Trisubstituted Purines. *Org. Lett.* **2006**, *8*, 5389–5392.

(29) Zhang, Q.; Li, J.; Shizu, K.; Huang, S.; Hirata, S.; Miyazaki, H.; Adachi, C. Design of Efficient Thermally Activated Delayed Fluorescence Materials for Pure Blue Organic Light Emitting Diodes. *J. Am. Chem. Soc.* **2012**, *134*, 14706–14709.

(30) Samanta, P. K.; Kim, D.; Coropceanu, V.; Bredas, J. L. Up-Conversion Intersystem Crossing Rates in Organic Emitters for Thermally Activated Delayed Fluorescence: Impact of the Nature of Singlet Vs Triplet Excited States. *J. Am. Chem. Soc.* **2017**, *139*, 4042–4051.

(31) Chen, J. X.; Xiao, Y. F.; Wang, K.; Sun, D.; Fan, X. C.; Zhang, X.; Zhang, M.; Shi, Y. Z.; Yu, J.; Geng, F. X.; Lee, C. S.; Zhang, X. H. Managing Locally Excited and Charge-Transfer Triplet States to Facilitate up-Conversion in Red TADF Emitters That Are Available for Both Vacuum- and Solution-Processes. *Angew. Chem., Int. Ed.* **2021**, *60*, 2478–2484.

(32) Wong, M. Y.; Zysman-Colman, E. Purely Organic Thermally Activated Delayed Fluorescence Materials for Organic Light-Emitting Diodes. *Adv. Mater.* **2017**, *29*, 1605444.

(33) Wex, B.; Kaafarani, B. R. Perspective on Carbazole-Based Organic Compounds as Emitters and Hosts in TADF Applications. *J. Mater. Chem. C* **2017**, *5*, 8622–8653.

(34) Murawski, C.; Leo, K.; Gather, M. C. Efficiency Roll-Off in Organic Light-Emitting Diodes. *Adv. Mater.* **2013**, *25*, 6801–6827.